



The following Communications have been judged by at least two referees to be “very important papers” and will be published online at [www.angewandte.org](http://www.angewandte.org) soon:

P. Mukhopadhyay, G. Zuber, P. Wipf, D. N. Beratan\*

**Contribution of a Chiral Solvent Imprint of a Solute to Optical Rotation**

J. Fölling, V. Belov, R. Kunetsky, R. Medda, A. Schönlé, A. Egner, C. Eggeling, M. Bossi, S. Hell\*

**Photochromic Rhodamines Provide Fluorescence Nanoscopy with Optical Sectioning**

O. Vendrell, F. Gatti, H.-D. Meyer\*

**Dynamics and Infrared Spectroscopy of the Protonated Water Dimer**

J. L. Stymiest, G. Dutheil, A. Mahmood, V. K. Aggarwal\*

**Lithiated Carbamates: Chiral Carbenoids for Iterative Homologation of Boranes and Boronic Esters**

M. Stępień, L. Latos-Grażyński, N. Sprutta, P. Chwalisz, L. Szterenberga

**Expanded Porphyrin With a Split Personality: A Hückel–Möbius Aromaticity Switch**

Z. Su, Y. Xu\*

**Hydration of a Chiral Molecule: the Gas-Phase Study of the Propylene Oxide–(Water)<sub>2</sub> Ternary Cluster**

Chemistry Unprotected

Anion Receptor Chemistry

Jonathan L. Sessler, Philip A. Gale, Won-Seob Cho

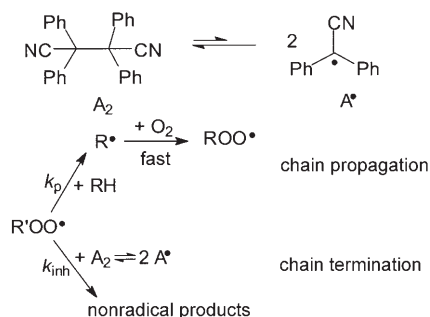
## Meeting Reviews

M. Köck,\* T. Lindel\* \_\_\_\_\_ 5268

## Books

reviewed by O. Reinaud \_\_\_\_\_ 5272

**Radical antioxidants:** Carbon-centered radicals, which exist in thermal equilibrium with their dimers in solution, show unexpectedly low reactivity with molecular oxygen. Nevertheless their high reactivity with peroxy radicals makes them a promising new class of chain-breaking antioxidants (see scheme).



## Highlights

### C Radicals

H.-G. Korth\* \_\_\_\_\_ 5274–5276

Carbon Radicals of Low Reactivity against Oxygen: Radically Different Antioxidants

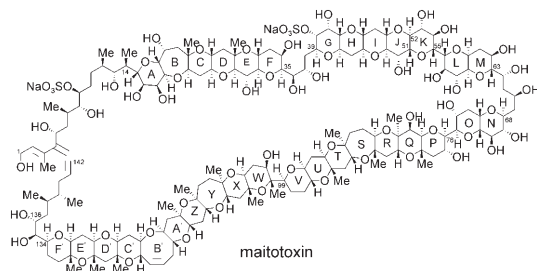
## Essays

### Structure Elucidation

K. C. Nicolaou,\*

M. O. Frederick \_\_\_\_\_ 5278–5282

On the Structure of Maitotoxin



**The right way round?** Biosynthetic considerations have put the reported structure of maitotoxin in doubt, in particular the stereochemistry of its J/K ring junction (C51/C52, see structure). Further consid-

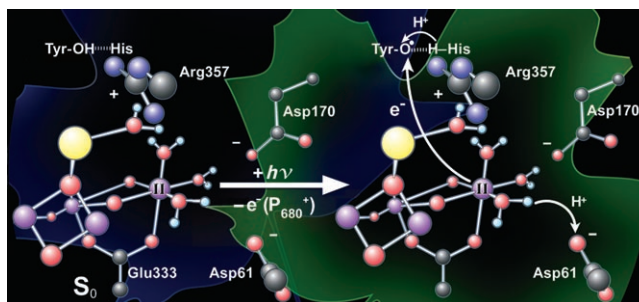
erations on the basis of computational techniques lead, however, to the conclusion that the originally proposed structure is most likely correct.

## Reviews

### Photosystem II

T. J. Meyer,\* M. H. V. Huynh,  
H. H. Thorp ————— 5284 – 5304

The Possible Role of Proton-Coupled  
Electron Transfer (PCET) in Water  
Oxidation by Photosystem II



**Wired for protons:** The absorption of light in green plants by photosystem II results in oxidation of water to oxygen at the oxygen-evolving complex (OEC). It is now possible to suggest an important role for proton-coupled electron transfer in this

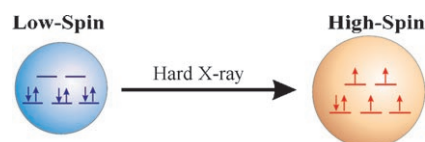
mechanism (see picture). Crucial overall in a complex sequence of reactions is a combination of coupled electron–proton transfer and long-range proton transfer by sequential local proton transfers.

## Communications

### Spin Crossover

G. Vankó,\* F. Renz,\* G. Molnár, T. Neisius,  
S. Kárpáti ————— 5306 – 5309

Hard-X-ray-Induced Excited-Spin-State  
Trapping



**All Xcited:** At low temperatures, an intense beam of hard X-rays excites photoswitchable molecular spin-crossover systems to generate metastable high-spin states (see picture). These states have spectroscopic properties similar to those of the states generated by light-induced excited-spin-state trapping. The new approach offers an excitation source with greater penetration.

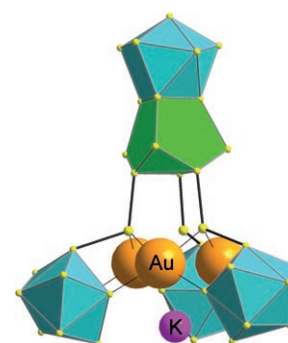
### Cluster Compounds

A. Spiekermann, S. D. Hoffmann,  
T. F. Fässler,\* I. Krossing,  
U. Preiss ————— 5310 – 5313



[Au<sub>3</sub>Ge<sub>45</sub>]<sup>9-</sup>—A Binary Anion Containing a  
{Ge<sub>45</sub>} Cluster

**The golden era of germanium:** The largest known germanium cluster [Au<sub>3</sub>Ge<sub>45</sub>]<sup>9-</sup> consists of 45 Ge atoms coordinated to three Au atoms and is obtained by the reaction of K<sub>4</sub>Ge<sub>9</sub> and [AuCl(PPh<sub>3</sub>)]. DFT calculations reveal the large variety of chemical-bond character in the {Ge<sub>45</sub>} moiety; localized two-center, two-electron bonds coexist with delocalized polyhedral and three-center, two-electron bonds.

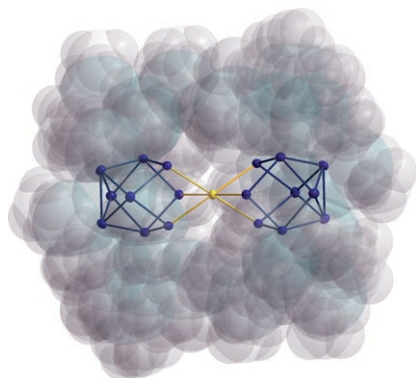


### For the USA and Canada:

ANGEWANDTE CHEMIE International  
Edition (ISSN 1433-7851) is published weekly  
by Wiley-VCH, PO Box 191161, 69451 Wein-  
heim, Germany. Air freight and mailing in the  
USA by Publications Expediting Inc., 200

Meacham Ave., Elmont, NY 11003. Periodicals  
postage paid at Jamaica, NY 11431. US POST-  
MASTER: send address changes to *Angewandte  
Chemie*, Wiley-VCH, 111 River Street, Hoboken,  
NJ 07030. Annual subscription price for insti-  
tutions: US\$ 5685/5168 (valid for print and

electronic / print or electronic delivery); for  
individuals who are personal members of a  
national chemical society prices are available  
on request. Postage and handling charges  
included. All prices are subject to local VAT/  
sales tax.



**Well-protected:** The first successful reaction with a metalloid cluster compound of Group 14 provides the new cluster species  $[\text{AuGe}_{18}\{\text{Si}(\text{SiMe}_3)_3\}_6]^-$  (see picture; Ge blue, Au yellow,  $\text{Si}(\text{SiMe}_3)_3$  groups are shown as a faded space-filling model), which can be considered as a first element on the way to a molecular cable.

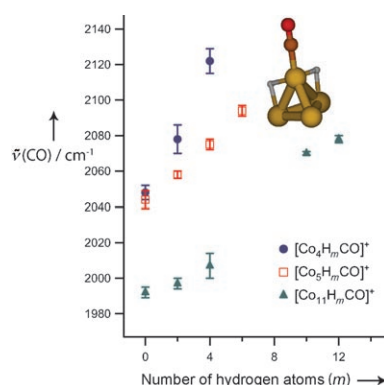
### Cluster Compounds

C. Schenk, A. Schnepf\* — 5314–5316

$[\text{AuGe}_{18}\{\text{Si}(\text{SiMe}_3)_3\}_6]^-$ : A Soluble Au–Ge Cluster on the Way to a Molecular Cable?



**H in control (of the electrons):** The bond strength of CO on small cationic cobalt clusters, as indicated by the C–O stretching band in the IR spectrum, can be precisely controlled by coadsorption of  $\text{H}_2$  molecules. Each coadsorbed H atom reduces the electron density available for back-donation by about 0.09–0.25 electrons, depending on cluster size.



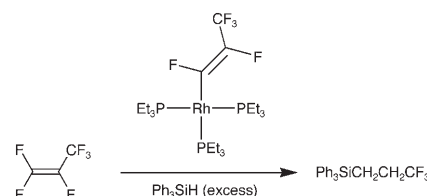
### Cluster Surface Chemistry

I. Swart, A. Fielicke,\* D. M. Rayner, G. Meijer, B. M. Weckhuysen, F. M. F. de Groot\* — 5317–5320

Controlling the Bonding of CO on Cobalt Clusters by Coadsorption of  $\text{H}_2$



**A clean break:** The novel catalytic conversion of hexafluoropropene into (3,3,3-trifluoropropyl)silanes by C–F activation has been developed (see scheme). The reactions are catalyzed by the rhodium complex  $[\text{Rh}\{(\text{Z})\text{-CF}=\text{CF}(\text{CF}_3)\}(\text{PEt}_3)_3]$ , proceed at room temperature, and are highly selective.



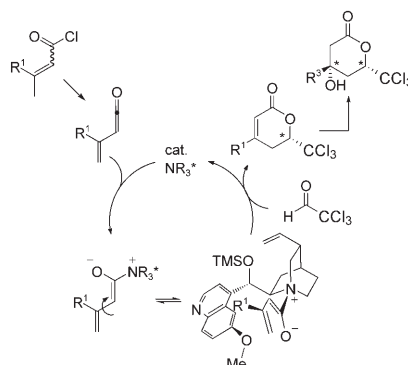
### Carbon–Fluorine Bond Activation

T. Braun,\* F. Wehmeier, K. Altenhöner — 5321–5324

Catalytic C–F Bond Activation of Hexafluoropropene by Rhodium: Formation of (3,3,3-Trifluoropropyl)silanes



**Smooth elaboration:** Versatile  $\delta$ -lactone building blocks are provided by tertiary-amine-catalyzed asymmetric [4+2] cycloadditions of  $\alpha,\beta$ -unsaturated acid chlorides and the electron-poor aldehyde chloral (see scheme). Silyl-substituted acid chlorides ( $\text{R}^1 = \text{R}_3\text{Si}$ ) can be used for the diastereoselective synthesis of  $\beta$ -hydroxy- $\delta$ -lactones possessing quaternary stereocenters.



### Asymmetric Cycloaddition

P. S. Tiseni, R. Peters\* — 5325–5328

Catalytic Asymmetric Formation of  $\delta$ -Lactones by [4+2] Cycloaddition of Zwitterionic Dienolates Generated from  $\alpha,\beta$ -Unsaturated Acid Chlorides



# Incredibly *inexpensive!*



Do chemistry journals really cost so much? Perhaps some do, but certainly not *Angewandte Chemie*! In 2007, an entire institution could subscribe through Wiley InterScience for about 4200 Euro and get access to 48 issues with over 1600 articles and all associated online search options, and for just 10% more, the printed issues could be included as well. For full members of the German Chemical Society (GDCh), a personal subscription cost less than 300 Euro, and student GDCh members paid only 140 Euro, which is just under 3 Euro per issue – a price that even compares with high-circulation newsstand publications!



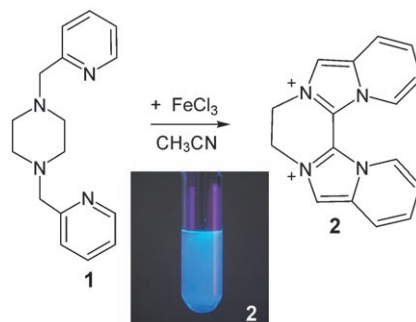
GESELLSCHAFT  
DEUTSCHER CHEMIKER



 **WILEY-VCH**

service@wiley-vch.de  
www.angewandte.org

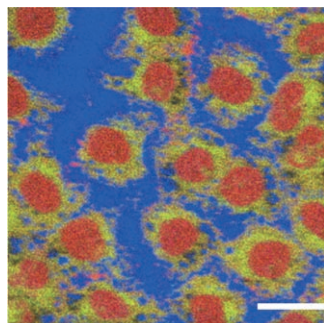
**When having the blues isn't so bad:** While normal coordination chemistry is observed when  $\text{FeCl}_3$  and the potential ligand **1** (see scheme) are mixed in dichloromethane, redox chemistry occurs in acetonitrile, which involves C–H activation and C–N bond formation, and finally leads to a water-soluble blue fluorophore **2**.



### Oxidations

M. Ostermeier, C. Limberg,\* B. Ziemer, V. Karunakaran — **5329–5331**

Solvent-Dependent Oxidation of a (Pyridylmethyl)amino Ligand by  $\text{FeCl}_3$  To Give a Water-Soluble Blue Fluorophore

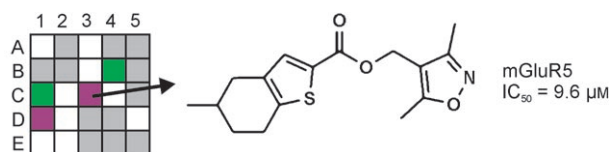


**A peek inside:** A  $\text{C}_{60}^+$  sputter ion source integrated into a time-of-flight secondary-ion mass spectrometer was used to dissect animal cells in a layer-by-layer fashion and analyze the spatial distribution of endogenous molecules. Repeated cycles of sputter erosion and SIMS analysis provided molecular information from the inside of the cells (see picture; red: amino acids, green: phospholipids, blue: glass substrate).

### Mass Spectrometry

D. Breitenstein, C. E. Rommel, R. Möllers, J. Wegener,\* B. Hagenhoff — **5332–5335**

The Chemical Composition of Animal Cells and Their Intracellular Compartments Reconstructed from 3D Mass Spectrometry



**No longer lost in space:** A virtual screening approach for the mapping of chemical space using supervised and unsupervised neural networks is presented. Novel scaffolds

of allosteric antagonists for mGluR 5 were identified in regions of chemical space that were not covered by active molecules from the training set.

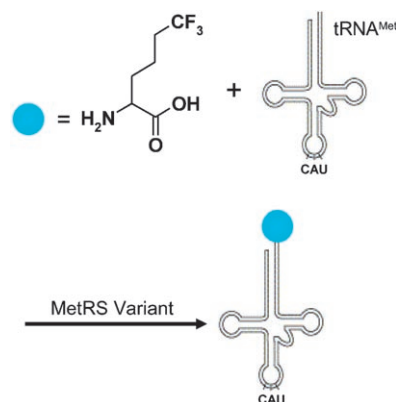
### Virtual Screening

S. Renner, M. Hechenberger, T. Noeske, A. Böcker, C. Jatzke, M. Schmuker, C. G. Parsons, T. Weil,\* G. Schneider\* — **5336–5339**

Searching for Drug Scaffolds with 3D Pharmacophores and Neural Network Ensembles



**A change for the better:** An efficient method for the identification of mutant methionyl-tRNA synthetases (MetRS) has been developed that enables global incorporation of noncanonical amino acids into recombinant proteins. By using the method, a MetRS variant has been identified that enables near-quantitative replacement of methionine by 6,6,6-trifluoronorleucine (see scheme).



### Protein Engineering

T. H. Yoo, D. A. Tirrell\* — **5340–5343**

High-Throughput Screening for Methionyl-tRNA Synthetases That Enable Residue-Specific Incorporation of Noncanonical Amino Acids into Recombinant Proteins in Bacterial Cells



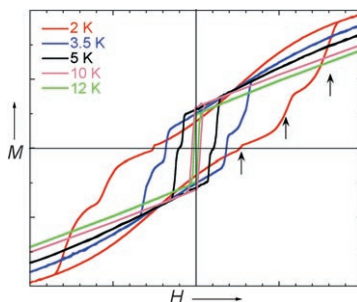


## Magnetic Properties

W. L. Queen, S.-J. Hwu,\*  
L. Wang — 5344–5347



A Low-Dimensional Iron(II) Phosphate Exhibiting Field-Dependent Magnetization Steps



**A step forward:** Large single crystals of the new magnetic solid  $\text{RbNa}_3\text{Fe}_7(\text{PO}_4)_6$  can be grown in a salt flux. Below the ferro-to-antiferromagnetic transition temperature of 6 K, the field ( $H$ ) dependence of the magnetization ( $M$ ) of an oriented crystal of the compound (see graph) exhibits equally spaced steps (arrows), which are probably a result of spin frustration.

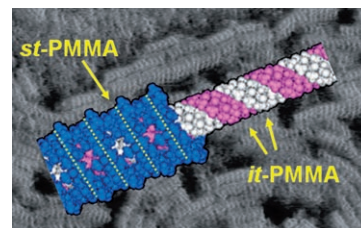
## Helical Structures

J. Kumaki,\* T. Kawauchi, K. Okoshi,  
H. Kusanagi, E. Yashima\* — 5348–5351



Supramolecular Helical Structure of the Stereocomplex Composed of Complementary Isotactic and Syndiotactic Poly(methyl methacrylate)s as Revealed by Atomic Force Microscopy

**A long-standing question** in polymer chemistry has been addressed by AFM, which revealed the helical conformation, handedness, and helical pitch (0.92 nm) of the title stereocomplex formed from a 1:2 mixture of the named polymers (*it*- and *st*-PMMA). The results provide convincing evidence for a triple-stranded helix (see structure against a background of the AFM image) as a plausible model for the stereocomplex.

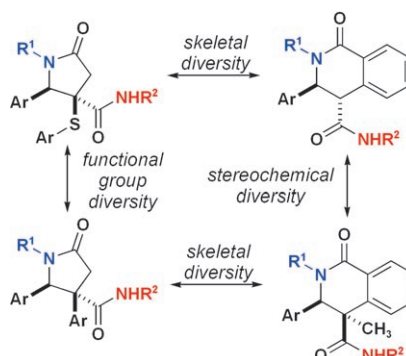


## Combinatorial Chemistry

P. Y. Ng, Y. Tang, W. M. Knosp,  
H. S. Stadler,\* J. T. Shaw\* — 5352–5355



Synthesis of Diverse Lactam Carboxamides Leading to the Discovery of a New Transcription-Factor Inhibitor



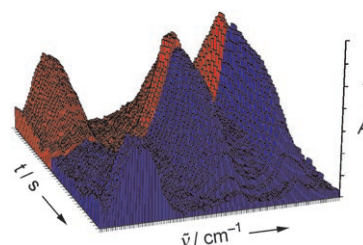
**Diversity is the key:** Skeletal diversity is a useful starting point in the search for compounds that modulate protein–biopolymer interactions. A library of 400 lactam carboxamides has been synthesized in a short synthetic sequence and a new compound that inhibits the interaction of a transcription factor (HOXA13) with its DNA target has been discovered, and inhibition of transcription is demonstrated in cells.

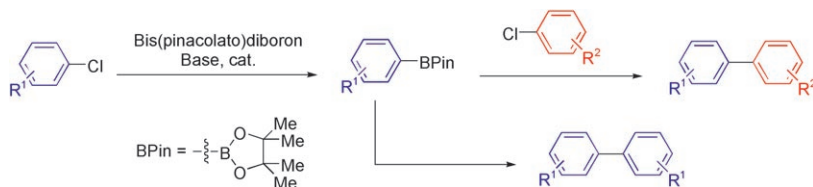
## Catalyst Structure

A. J. Dent, J. Evans,\* S. G. Fiddy, B. Jyoti,  
M. A. Newton, M. Tromp — 5356–5358

Rhodium Dispersion during NO/CO Conversions

**Change and change again:** Under catalytic conditions for NO/CO conversion, simultaneous time-resolved extended X-ray absorption fine structure spectroscopy and IR studies show that the rhodium atoms in 5 wt%  $\text{Rh}/\text{Al}_2\text{O}_3$  rapidly migrate between CO-covered Rh particles and mononuclear Rh–NO sites depending on the changing gas composition. At lower temperatures (473 K), there is interconversion between mononuclear  $\text{Rh}(\text{CO})_2$  and  $\text{Rh}(\text{NO})$  centers.





**From chloride to boronate:** Catalysts comprising palladium and biaryl mono-phosphine ligands provide highly active systems for the borylation of aryl and heteroaryl chlorides (see scheme). Symmetrical and unsymmetrical biaryl pro-

ducts can also be prepared directly from two aryl chlorides without isolation of the intermediate boronate esters. Computational studies provide insight into the roles of the biaryl phosphine ligand and the KOAc base in the catalytic cycle.

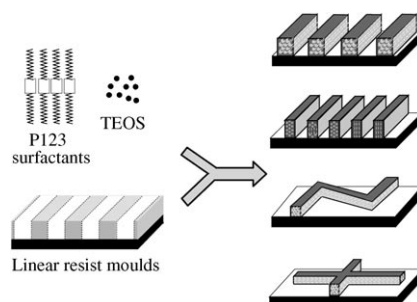
## C-C Coupling

K. L. Billingsley, T. E. Barder,  
S. L. Buchwald\* 5359–5363

Palladium-Catalyzed Borylation of Aryl Chlorides: Scope, Applications, and Computational Studies



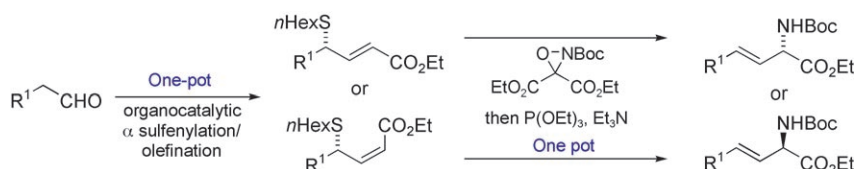
**A top-down/bottom-up approach** has been developed to fabricate mesoporous silica with well-aligned mesochannels of controlled orientation by means of cooperative assembly of an amphiphilic tri-block copolymer (P123) and silica species within lithographically designed confined nanospaces. Some mesochannel patterns that can be prepared by this technique are shown schematically in the picture. TEOS = tetraethoxysilane.



## Mesoporous Materials

C.-W. Wu, T. Ohsuna, T. Edura,  
K. Kuroda\* 5364–5368

Oriental Control of Hexagonally Packed Silica Mesochannels in Lithographically Designed Confined Nanospaces



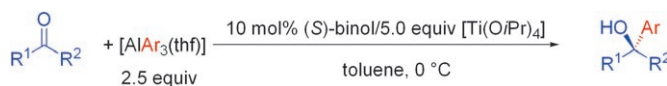
**Have it both ways:** Enantiomerically enriched *E* vinyl glycines may be accessed from aldehydes in a concise sequence that combines an organocatalytic  $\alpha$  sulfenylation, stereoselective olefination, a sulfimide, and a [2,3] sigmatropic rear-

rangement (see scheme, Boc = *tert*-butoxycarbonyl, *n*Hex = *n*-hexyl). Either enantiomeric series can be accessed by control of the alkene geometry in the olefination step.

## Asymmetric Synthesis

A. Armstrong,\* L. Challinor,  
J. H. Moir 5369–5372

Exploiting Organocatalysis: Enantioselective Synthesis of Vinyl Glycines by Allylic Sulfimide [2,3] Sigmatropic Rearrangement



**Chiral transfer:** Novel asymmetric aryl transfers from  $[AlAr_3(thf)]$  to a wide variety of ketones are catalyzed by an in situ generated titanium species with

(*S*)-binol as the chiral ligand. The reaction affords tertiary alcohols with enantioselectivities up to 97% *ee* (see scheme). Binol = 2,2'-dihydroxy-1,1'-binaphthyl.

## Asymmetric Arylation

C.-A. Chen, K.-H. Wu,  
H.-M. Gau\* 5373–5376

Highly Enantioselective Aryl Additions of  $[AlAr_3(thf)]$  to Ketones Catalyzed by a Titanium(IV) Catalyst of (*S*)-Binol

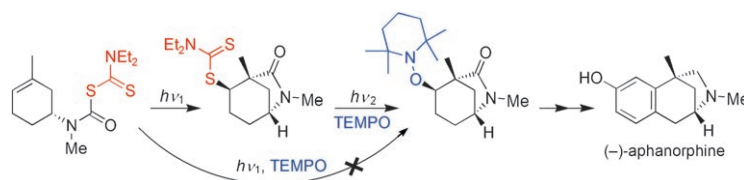


## Alkaloid Synthesis

R. S. Grainger,\* E. J. Welsh 5377–5380



Formal Synthesis of (–)-Aphanorphine Using Sequential Photomediated Radical Reactions of Dithiocarbamates



**Time to change the light bulb:** An alkyl dithiocarbamate, itself formed through a photoinitiated group-transfer cyclization of a carbamoyl radical, undergoes a second photomediated radical process initiated with a different light source.

These two reactions, which proceed through the same cyclohexenyl radical intermediate, are key steps in a new asymmetric synthesis of the alkaloid aphanorphine. TEMPO = 2,2,6,6-tetramethyl-1-piperidinoxyl radical.

## Ligand Immobilization

G. Hamasaka, A. Ochida, K. Hara, R. Sawamura\* 5381–5383



Monocoordinating, Compact Phosphane Immobilized on Silica Surface: Application to Rhodium-Catalyzed Hydrosilylation of Hindered Ketones

**Activity without mobility:** A compact trialkylphosphane, chemically immobilized on a silica gel surface (see picture), exhibited unique coordination behavior to form a 1:1 Rh/P complex. The monophosphane–{RhCl(cod)} species on the surface was highly active for catalysis of the hydrosilylation of ketones, allowing the conversion of di(*tert*-butyl) ketone into the corresponding TBS-protected alcohol. TBS = *tert*-butyldimethylsilyl; cod = 1,5-cyclooctadiene.

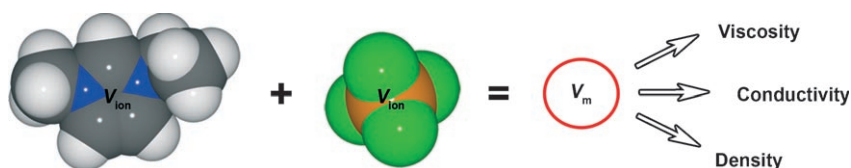


## Ionic Liquids

J. M. Slattery,\* C. Daguenet, P. J. Dyson, T. J. S. Schubert, I. Krossing\* 5384–5388



How to Predict the Physical Properties of Ionic Liquids: A Volume-Based Approach



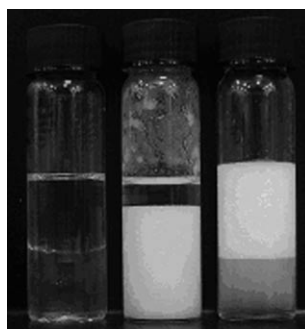
**The molecular volume  $V_m$**  (that is, the sum of the ionic volumes  $V_{ion}$  of the constituent ions) of an ionic liquid (IL) in combination with an anion-dependent empirical relationship is all one needs to predict

physical properties such as viscosity, conductivity, and density of  $[N(CN)_2]^+$ ,  $[BF_4]^-$ ,  $[PF_6]^-$ , and  $[N(SO_2CF_3)_2]^+$  ionic liquids, including those which may as yet only exist on paper.

## Emulsions

B. P. Binks,\* J. A. Rodrigues 5389–5392

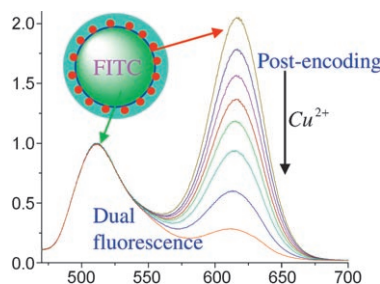
Double Inversion of Emulsions By Using Nanoparticles and a Di-Chain Surfactant



**Two shakes:** Double phase inversion of emulsions stabilized by a mixture of silica nanoparticles and a di-chain cationic surfactant can be induced by surfactant concentration alone. The picture shows emulsions of dodecane and water stabilized by silica nanoparticles (left, unstable), di-chain cationic surfactant (right, oil-in-water), and a mixture of the two (middle, water-in-oil).



**Dual control:** Hybrid silica–nanocrystal–organic dye superstructures comprising fluorescein isothiocyanate (FITC)-doped silica cores, embedded CdTe quantum dots, and an outer silica shell display well-resolved dual fluorescence emission. Multicolor encoding fluorescent probes are generated by modulating the fluorescence intensity ratio of the dual emission by a simple post-encoding strategy (see picture).



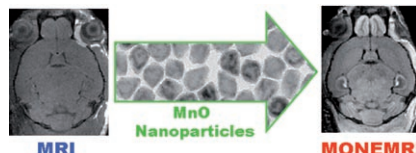
### Fluorescent Probes

C. Wu, J. Zheng, C. Huang, J. Lai, S. Li, C. Chen, Y. Zhao\* — 5393 – 5396

Hybrid Silica–Nanocrystal–Organic Dye Superstructures as Post-Encoding Fluorescent Probes



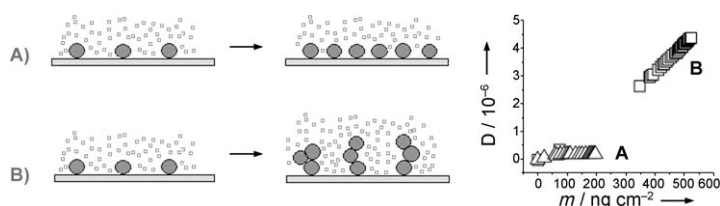
**Contrasting images:** A new  $T_1$  contrast agent for magnetic resonance imaging (MRI) based on MnO nanoparticles reveals a bright signal enhancement and fine anatomic structures in the  $T_1$ -weighted MR image of a mouse brain (see picture; left MRI, right MnO-enhanced MRI (MONEMRI)). Furthermore, MnO nanoparticles conjugated with a tumor-specific antibody were used for selectively imaging breast cancer cells in a metastatic tumor in brain.



### Imaging Agents

H. B. Na, J. H. Lee,\* K. An, Y. I. Park, M. Park, I. S. Lee, D.-H. Nam, S. T. Kim, S.-H. Kim, S.-W. Kim, K.-H. Lim, K.-S. Kim, S.-O. Kim, T. Hyeon\* — 5397 – 5401

Development of a  $T_1$  Contrast Agent for Magnetic Resonance Imaging Using MnO Nanoparticles



**Covering up:** The greater ability of anti-freeze proteins (AFPs), relative to polyvinyl pyrrolidone (PVP), to inhibit the reformation of gas hydrates, despite their smaller adsorption mass, has been explained by using a quartz crystal

microbalance equipped with the ability to measure the dissipation factor ( $D$ ). Whereas AFPs can form a rigid and compact film on the nucleating surface (A), PVP forms a porous and loose film (B).

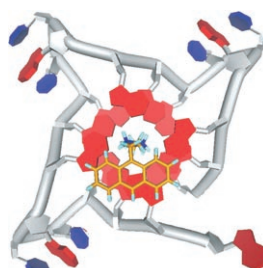
### Surface Chemistry

H. Zeng, V. K. Walker, J. A. Ripmeester\* — 5402 – 5404

Approaches to the Design of Better Low-Dosage Gas Hydrate Inhibitors



**Under control:** An anthracene polyammonium derivative induces folding of the highly polymorphic human telomeric DNA into a single parallel G-quadruplex conformer through an unusual mode of interaction. The sequential use of this ligand and a porphyrazine allows controlled conformational switching of the quadruplex between parallel and antiparallel conformations.



### DNA Folding

R. Rodriguez, G. D. Pantoş, D. P. N. Gonçalves, J. K. M. Sanders, S. Balasubramanian\* — 5405 – 5407

Ligand-Driven G-Quadruplex Conformational Switching By Using an Unusual Mode of Interaction

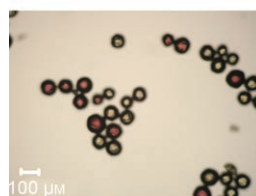


## Substrate specificity of kinase

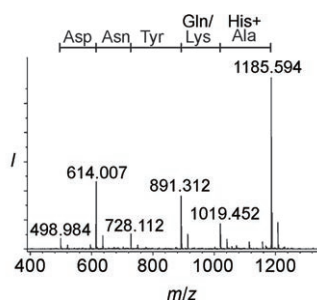
Y.-G. Kim, D.-S. Shin, E.-M. Kim, H.-Y. Park,  
C.-S. Lee, J.-H. Kim, B.-S. Lee, Y.-S. Lee,  
B.-G. Kim\* ————— 5408 – 5411



High-Throughput Identification of Substrate Specificity for Protein Kinase by Using an Improved One-Bead-One-Compound Library Approach



MALDI-TOF-MS



**Pick and choose:** The identification of the substrate specificity of a protein kinase is critical in understanding its role and function in a cellular signal transduction network. A high-throughput platform was

developed for the identification of tyrosine kinase substrate specificity by using an improved one-bead-one-compound ladder peptide library and MALDI-TOF MS.

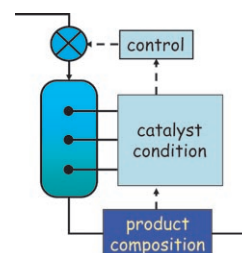
## Heterogeneous Catalysis

S. M. Bennici, B. M. Vogelaar, T. A. Nijhuis,  
B. M. Weckhuysen\* ————— 5412 – 5416



Real-Time Control of a Catalytic Solid in a Fixed-Bed Reactor Based on In Situ Spectroscopy

**A reality check:** Reactor control by online spectroscopy is illustrated for a  $\text{Cr}/\text{Al}_2\text{O}_3$  alkane dehydrogenation catalyst and a vanadium phosphorus oxide catalyst used in the selective oxidation of *n*-butane to maleic anhydride. Rather than testing the product composition alone, the methodology monitors the state of the catalyst in the reactor, and changes the reaction conditions to keep the catalyst in its optimal state (see picture).

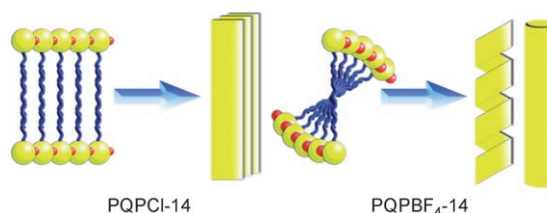


## Nanostructures

D. Wu, L. Zhi,\* G. J. Bodwell, G. Cui,  
N. Tsao, K. Müllen\* ————— 5417 – 5420



Self-Assembly of Positively Charged Discotic PAHs: From Nanofibers to Nanotubes



**Mind your PQPs:** 1D nanostructures were fabricated by the self-assembly of amphiphilic centrally charged discotic 9-alkyl-2-phenylbenzo[8,9]quinolizino[4,5,6,7-*fed*]-phenanthridinium (PQP) salts. Increasing the alkyl chain length of the PQP salts

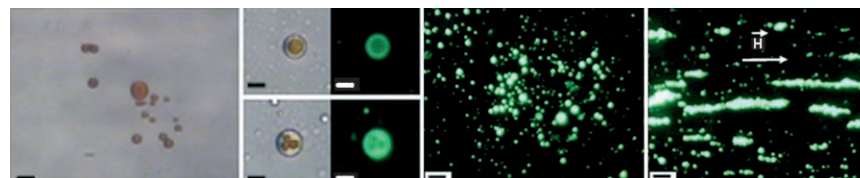
resulted in nanoscaled lamellar structures, whereas changing the counterion of the PQP salts from  $\text{Cl}^-$  to  $\text{BF}_4^-$  led to a change from nanoribbons to helices and tubes.

## Hybrid Vesicles

G. Beaune, B. Dubertret, O. Clément,  
C. Vayssettes, V. Cabuil,  
C. Ménager\* ————— 5421 – 5424

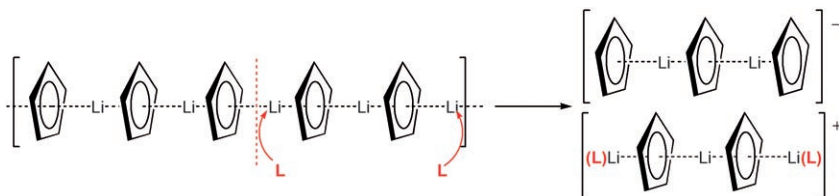


Giant Vesicles Containing Magnetic Nanoparticles and Quantum Dots: Feasibility and Tracking by Fiber Confocal Fluorescence Microscopy



**Hybrid vesicles:** Magnetic nanoparticles ( $\gamma\text{-Fe}_2\text{O}_3$ ) and quantum dots ( $\text{CdSe}/\text{ZnS}$ ) can be entrapped in stable vesicles by emulsion processes. The hybrid vesicles (HVs) have distinct magnetic and fluo-

rescence properties (see images; scale bars: 10  $\mu\text{m}$ ). Fluorescence detection allows magnetic manipulation and tracking of the HVs in vivo by both magnetic resonance and fluorescence imaging.



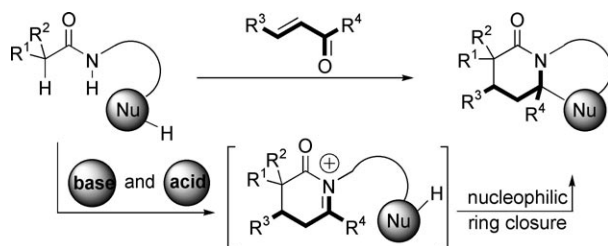
### Cyclopentadienyl Ligands

C. Fernández-Cortabitarte, F. García,  
J. V. Morey, M. McPartlin, S. Singh,  
A. E. H. Wheatley,\*  
D. S. Wright\* 5425 – 5427

**Breaking up:** The first triple-decker sandwich anion  $[(\eta^5\text{-Cp})\text{Li}(\eta^5\text{-Cp})\text{Li}(\eta^5\text{-Cp})]^-$  of lithocene ( $\text{Cp} = \text{C}_5\text{H}_5$ ) (observed in the charge-separated complex  $[(\text{L})\text{Li}(\mu\text{-Cp})\text{Li}(\mu\text{-Cp})\text{Li}(\text{L})]^+[(\eta^5\text{-Cp})\text{Li}(\eta^5\text{-Cp})\text{Li}(\eta^5\text{-Cp})]^-$ ) is formed in the reaction of  $[\text{Cp}_2\text{V}]$

with  $\text{hppLi}$  ( $\text{hppH} = 1,3,4,6,7,8\text{-hexahydro-}2H\text{-pyrimido}[1,2-a]\text{pyrimidine}$ ). The  $\text{V}\equiv\text{V}$ -bonded complex  $[\text{V}_2(\text{hpp})_4]$  ( $\text{L}$ ) effectively acts as a ligand to intercept the polymeric structure of  $[\text{CpLi}]_\infty$  (see scheme).

Trapping of Oligomeric  
Cyclopentadienyllithium Cationic and  
Anionic Fragments by a  $\text{V}\equiv\text{V}$ -Bonded  
Ligand



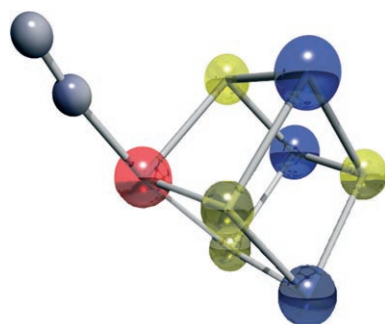
**One thing leads to another:** Site-isolated base and acid catalysts have been exploited in Michael addition, *N*-acyl iminium ion cyclization cascades with amide pronucleophiles and  $\alpha,\beta$ -unsaturated car-

bonyl compounds. The reaction sequence has broad scope, uses commercially available catalysts, is atom efficient, and can be scaled by way of a flow-reactor setup.

### Michael Addition

A. W. Pilling, J. Boehmer,  
D. J. Dixon\* 5428 – 5430

Site-Isolated Base- and Acid-Mediated  
Michael-Initiated Cyclization Cascades

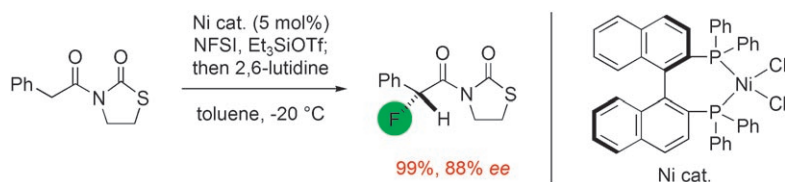


**An end-on N<sub>2</sub> ligand** is the outstanding feature in  $[(\eta^5\text{-C}_5\text{Me}_5)\text{Ir}]_3\{\text{Ru}(\text{tmeda})\text{-}(\text{N}_2)\}(\mu_3\text{-S})_4]$  ( $\text{tmeda} = \text{Me}_2\text{NCH}_2\text{CH}_2\text{-NMe}_2$ ), the first cubane-type metal sulfido cluster with a dinitrogen ligand, which has been isolated and fully characterized by single-crystal X-ray analysis. The picture shows the cluster core with the Ru-bound N<sub>2</sub> ligand (Ir blue, N gray, Ru red, S yellowish green).

### Nitrogen Fixation

H. Mori, H. Seino, M. Hidai,  
Y. Mizobe\* 5431 – 5434

Isolation of a Cubane-Type Metal Sulfido  
Cluster with a Molecular Nitrogen Ligand



**Not binary, but trinary:** A binary system consisting of  $\text{Ni}(\text{OTf})_2$ -binap complex and 2,6-lutidine failed to promote the asymmetric fluorination of ester equivalents. However, upon the addition of a substoichiometric amount of Et<sub>3</sub>SiOTf to

the  $\text{NiCl}_2$ -binap/2,6-lutidine catalyst, the monofluorinated products were obtained in good yield with high enantioselectivity (see example). NFSI = *N*-fluorobenzene-sulfonamide, Tf = trifluoromethane-sulfonyl.

### Asymmetric Catalysis

T. Suzuki, Y. Hamashima,  
M. Sodeoka\* 5435 – 5439

Asymmetric Fluorination of  $\alpha$ -Aryl Acetic  
Acid Derivatives with the Catalytic System  
 $\text{NiCl}_2$ -Binap/ $\text{R}_3\text{SiOTf}$ /2,6-Lutidine

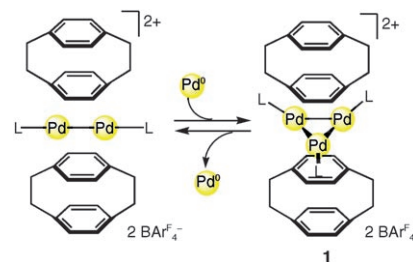
## Sandwich Complexes

T. Murahashi,\* M. Fujimoto, Y. Kawabata,  
R. Inoue, S. Ogoshi,  
H. Kurosawa \_\_\_\_\_ **5440–5443**



Discrete Triangular Tripalladium  
Sandwich Complexes of Arenes

**Sandwich triangles:** A bis([2.2]paracyclophane)tripalladium complex (**1**) was isolated and characterized by NMR spectroscopy, and a mixed-ligand derivative was structurally characterized. These complexes are the first isolated  $\mu_3$ -arene trimetal complexes of a Group 10 metal. Complex **1** undergoes facile release of a  $\text{Pd}^0$  atom (see scheme) and as such may be regarded as a  $\text{Pd}^0$  reservoir.



Supporting information is available on the WWW  
(see article for access details).



A video clip is available as Supporting Information  
on the WWW (see article for access details).

**Angewandte Chemie International Edition**  
WILEY-INTERSCIENCE®  
DISCOVER SOMETHING GREAT

„Hot Papers“ werden von der Redaktion wegen ihrer Bedeutung für ein aktuelles Gebiet der Chemie ausgewählt. Eine Vorschau mit den Inhaltsverzeichniseinträgen dieser Artikel finden Sie auf der Homepage der *Angewandten Chemie* unter [www.angewandte.de](http://www.angewandte.de) in Wiley InterScience.

Alle Beiträge in der *Angewandten Chemie* erscheinen online mehrere Wochen vor dem gedruckten Heft. Sie finden Sie unter dem Link „EarlyView“ auf der Angewandten-Homepage in Wiley InterScience.

**Angewandte**

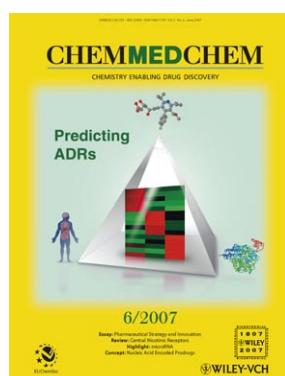
## Service

**Spotlights on Angewandte's  
Sister Journals** \_\_\_\_\_ **5264–5265**

**Keywords** \_\_\_\_\_ **5444**

**Authors** \_\_\_\_\_ **5445**

**Preview** \_\_\_\_\_ **5447**



**For more information on  
ChemMedChem see  
[www.chemmedchem.org](http://www.chemmedchem.org)**

## Corrigenda

The concentrations of peptide used in the studies in this Communication were incorrectly quoted. All A $\beta$  concentrations should be multiplied by a factor of 10; that is, [Cu<sup>2+</sup>]/[A $\beta$ ] = 1, 4, and 6 (instead of 0.1, 0.4, and 0.6, respectively). The authors apologize for the oversight but point out that the ESR and TEM results still demonstrate a correlation between the specific Cu<sup>2+</sup> ion coordination and the overall morphology of aggregates.

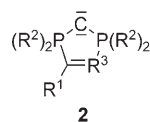
The Aggregated State of Amyloid- $\beta$  Peptide In Vitro Depends on Cu<sup>2+</sup> Ion Concentration

S. Jun, S. Saxena\* — 3959–3961

*Angew. Chem. Int. Ed.* **2007**, 46

DOI 10.1002/anie.200700318

In this Communication, the substituent labels for P-heterocyclic carbodiphosphoranes **2** (Scheme 2) were incorrectly shown and incorrectly listed in Table 1 for the proton affinities. The correct structure of **2** is shown below, along with the revised part of Table 1 corresponding to **2**. The authors apologize for the oversight but point out that their conclusions are not affected by this error.



Carbodiphosphoranes: The Chemistry of Divalent Carbon(0)

R. Tonner, F. Öxler, B. Neumüller,\*  
W. Petz,\* G. Frenking\* — 8038–8042

*Angew. Chem. Int. Ed.* **2006**, 45

DOI 10.1002/anie.200602552

**Table 1:** Calculated (RI-MP2/TZVPP//RI-BP86/SVP) first and second proton affinities (PAs) in kcal mol<sup>−1</sup>.

	P-heterocyclic CDPs			1st PA	2nd PA
	R <sup>1</sup>	R <sup>3</sup>	R <sup>2</sup>		
<b>2a</b>	H	N	H	251.5	110.5
<b>2b</b>	H	N	Me	270.8	143.3
<b>2c</b>	H	N	NH <sub>2</sub>	271.4	138.1
<b>2d</b>	H	N	NMe <sub>2</sub>	275.3	157.8
<b>2e</b>	Me	N	NMe <sub>2</sub>	277.6	160.3
<b>2f</b>	Ph	N	NiPr <sub>2</sub>	284.2	188.3
<b>2g</b>	Ph	N	NiPr <sub>2</sub> , iPr <sub>2</sub> N(CH <sub>2</sub> ) <sub>2</sub> NiPr <sub>2</sub>	284.5	179.0
	R <sup>2</sup>	R <sup>3</sup>	R <sup>1</sup>		
<b>2h</b>	H	CH	H	261.8	119.1
<b>2i</b>	H	CH	Me	278.2	149.7
<b>2k</b>	H	CH	NH <sub>2</sub>	277.5	144.6
<b>2l</b>	H	CH	NMe <sub>2</sub>	280.0	162.6
<b>2m</b>	Me	CH	NiPr <sub>2</sub>	287.3	190.5

## Retraction

After the online publication of this Communication (March 30, 2007), it has been brought to the authors' attention that the <sup>13</sup>C NMR spectra of the assumed azepinoazepine synthesized are essentially identical to those of the viologen structure.<sup>[1]</sup> <sup>1</sup>H NMR spectra also support this finding, although they were measured in different solvents and at different field strengths.<sup>[2]</sup> The authors therefore retract this Communication and apologize for any inconvenience.

Ring Expansion of a 4,4'-Bipyridyl Derivative into  $\pi$ -Conjugated Azepinoazepines

I. Yamaguchi,\* S. Tsutsui, M. Sato

[1] W. W. Porter III, T. P. Vaid, *J. Org. Chem.* **2005**, 70, 5028.

[2] H. Kamogawa, S. Sato, *Bull. Chem. Soc. Jpn.* **1991**, 64, 321.

DOI 10.1002/anie.200700170



# Ring Expansion of a 4,4'-Bipyridyl Derivative into $\pi$ -Conjugated Azepinoazepines\*\*

Isao Yamaguchi,\* Saori Tsutsui, and Moriyuki Sato

Azepine derivatives fused with aromatic rings represent an important class of compounds as they display potential or proven pharmacologic activity.<sup>[1]</sup> A large number of reports on synthetic approaches towards these compounds have been published.<sup>[2]</sup> Metal-complex-catalyzed intramolecular cyclization reactions are useful for the synthesis of azepine derivatives fused with aromatic rings such as benzene, imidazole, and pyridine rings.<sup>[3]</sup> However, these cyclization reactions sometimes cause undesirable side reactions. Ring-expansion reactions are also utilized for the preparation of azepine derivatives, and they proceed without side reactions.<sup>[4]</sup> It has been reported that the photolysis of diazo-naphthalenes causes ring expansion to yield azepinoazepines.<sup>[4d]</sup> These azepinoazepines are not fully unsaturated, and attempts to convert them into fully unsaturated diazaheptalene have been unsuccessful. Fully unsaturated azepinoazepine should show interesting optical and electrochemical properties as a result of its  $\pi$ -conjugated electron system. To the best of our knowledge, there has been only one report on the azepinoazepines<sup>[4d]</sup> and fully unsaturated azepinoazepines have not been prepared so far.

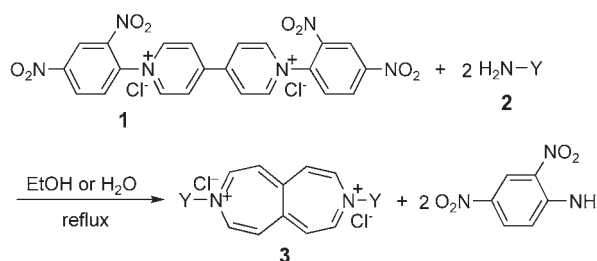
Recently, we reported the ring expansion of the pyridyl group of *N*-(2,4-dinitrophenyl)pyridinium chloride into diaza[12]annulene by reaction with an amine.<sup>[5]</sup> According to this reaction, the reaction of 1,1'-bis(2,4-dinitrophenyl)-4,4'-bipyridinium dichloride (**1**) with an amine may provide a diaza[12]annulene dimer. However, we found that the reaction yields unexpected products, namely *N*-substituted azepinoazepines. These products are a new type of azepine derivative with an expanded  $\pi$ -conjugation system.

Organic reactions in aqueous media have received considerable attention because of their potential advantages with regard to costs, safety, and environmental concerns.<sup>[6]</sup> In contrast to many reports on organic reactions in mixtures of water and organic solvents, organic syntheses in water, except for simple hydrolysis reactions, are limited as a result of the poor solubility of organic reactants in water. Compound **1** and certain amines used as starting materials in this work are

soluble in water, and the previously reported reaction of water-soluble *N*-(2,4-dinitrophenyl)pyridinium chloride with amines proceeds smoothly in water to provide *N*-substituted diaza[12]annulene through ring expansion of the pyridyl group. These results urged us to carry out the reaction of **1** with amines in water.

Herein, we report the results of the reaction of **1** with various amines **2** in ethanol and water, as well as the structures and optical and electrochemical properties of the obtained azepinoazepines **3**. A plausible reaction pathway is also proposed.

Reaction of **1** with substituted amines **2** (1:2) in refluxing EtOH (Scheme 1) gave rise to *N*-substituted azepinoazepine dichlorides **3**. Use of water-soluble amines **2a–2d** under



**Scheme 1.** Reaction of 1,1'-bis(2,4-dinitrophenyl)-4,4'-bipyridinium dichloride (**1**) with amines **2**. See Table 1 for Y groups.

aqueous conditions also yielded the azepinoazepines **3a–3d**. The results of these reactions are summarized in Table 1. The obtained azepinoazepines **3** were soluble in water and in organic solvents such as methanol, *N,N*-dimethylformamide, and dimethyl sulfoxide. Their structures were determined by FAB mass spectrometry, <sup>1</sup>H and <sup>13</sup>C NMR spectroscopy, and elemental analysis.

Figure 1 depicts the <sup>1</sup>H NMR spectra of **3d–3g** in D<sub>2</sub>O. Peaks at approximately  $\delta$  = 9.3 and 8.7 ppm are assigned to H<sup>a</sup> and H<sup>b</sup> of the azepinoazepine ring, respectively. The observation of the two signals of the azepinoazepine ring suggests that  $\pi$  electrons are delocalized along the azepinoazepine ring, as shown in Figure 1. <sup>13</sup>C NMR spectroscopy data also support this view, showing three signals attributed to the azepinoazepine ring.<sup>[7]</sup> The <sup>1</sup>H NMR peak positions of the azepinoazepine ring of **3a–3h** are essentially the same, independent of the structure of the *N* substituents. The difference in the chemical shifts between the two halophenyl hydrogen atoms H<sup>c</sup> and H<sup>d</sup> of **3d**, **3f**, and **3g** are  $\delta$  = 0.38, 0.11, and 0.57 ppm, respectively, whereas the two signals of chlorophenyl hydrogen atoms of **3e** are located at essentially the same position. These data suggest that the azepinoazepine

[\*] Prof. Dr. I. Yamaguchi, S. Tsutsui, Prof. Dr. M. Sato  
Department of Material Science  
Faculty of Science and Engineering  
Shimane University  
1060 Nishikawatsu, Matsue 690-8504 (Japan)  
Fax: (+81) 852-32-6421  
E-mail: iyamaguchi@riko.shimane-u.ac.jp

[\*\*] The authors wish to thank Prof. Dr. T. Yamamoto and Dr. H. Fukumoto (Tokyo Institute of Technology) for help with mass spectrometry measurements.

Supporting information for this article is available on the WWW under <http://www.angewandte.org> or from the author.

**Table 1:** Reaction of 1,1'-bis(2,4-dinitrophenyl)-4,4'-bipyridinium dichloride **1** with amines **2**.<sup>[a]</sup>

Entry	Y (amine)	<b>2</b>	Solvent	Product	Yield [%] <sup>[b]</sup>
1	C <sub>6</sub> H <sub>5</sub>	<b>2a</b>	EtOH	<b>3a</b>	91
2			H <sub>2</sub> O		75
3	4-MeOC <sub>6</sub> H <sub>4</sub>	<b>2b</b>	EtOH	<b>3b</b>	90
4			H <sub>2</sub> O		69
5	2,5-MeC <sub>6</sub> H <sub>3</sub>	<b>2c</b>	EtOH	<b>3c</b>	84
6			H <sub>2</sub> O		45
7	4-FC <sub>6</sub> H <sub>4</sub>	<b>2d</b>	EtOH	<b>3d</b>	91
8			H <sub>2</sub> O		71
9	4-ClC <sub>6</sub> H <sub>4</sub>	<b>2e</b>	EtOH	<b>3e</b>	78
10	4-BrC <sub>6</sub> H <sub>4</sub>	<b>2f</b>	EtOH	<b>3f</b>	88
11	4-IC <sub>6</sub> H <sub>4</sub>	<b>2g</b>	EtOH	<b>3g</b>	84
12	<i>p</i> -terphenyl	<b>2h</b>	EtOH	<b>3h</b>	95
13	<i>n</i> -hexyl	<b>2i</b>	EtOH	<b>3i</b>	38

[a] A solution of **1** and **2** in 1:2 molar ratio in either ethanol (entries 1, 3, 5, 7, and 9–13) or water (entries 2, 4, 6, and 8) was heated at reflux for 12 h under nitrogen (see Scheme 1 for details). [b] Yield of isolated product.

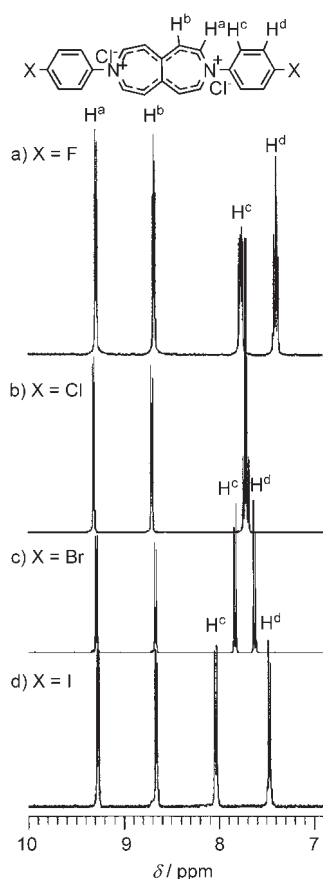


**Figure 1.** <sup>1</sup>H NMR spectra of **3d–3g** in D<sub>2</sub>O.

ring has an electron-withdrawing property similar to that of the chloro group.

The absorption peaks of **3** are influenced by the structures of the N substituents, as summarized in Table 2. Azepinoazepine dichloride **3h** with *p*-terphenyl substituents shows absorptions at longer wavelengths as compared to the other

**Table 2:** Absorption and electrochemical data for azepinoazepines **3**.

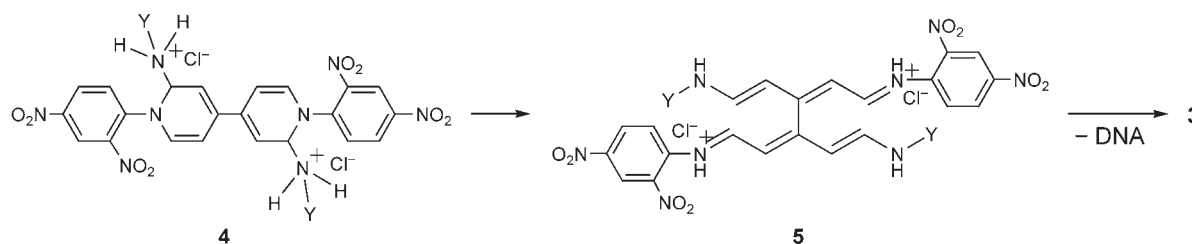
Entry	<b>3</b>	$\lambda_{\text{max}}$ <sup>[a]</sup> [nm] (log $\epsilon$ )	$E_{\text{pc}}(1), E_{\text{pc}}(2)$ [V] <sup>[b]</sup>	$E_{\text{pa}}(1), E_{\text{pa}}(2)$ [V] <sup>[b]</sup>
1	<b>3a</b>	245 (4.11), 320 (4.49)	−1.53	−0.48, 0
2	<b>3b</b>	253 (4.26), 380 (4.67)	−1.51	−0.84, −0.45
3	<b>3c</b>	255 (4.05), 268 (4.07), 299 (3.97)	−1.84	−0.92, −0.44
4	<b>3d</b>	255 (4.02), 299 (4.09), 321 (4.08)	−1.48	−0.57, −0.05
5	<b>3e</b>	259 (4.12), 290 (4.13), 326 (4.16)	−1.23, −1.74	−1.10, −0.61
6	<b>3f</b>	254 (4.05), 329 (4.19)	−1.17, −1.73	−1.11, −0.13
7	<b>3g</b>	240 (4.07), 342 (4.27)	−1.06, −1.88	−0.15
8	<b>3h</b>	289 (4.35), 385 (3.99)	−1.47	−0.88, −0.31
9	<b>3i</b>	261 ( $\approx$ 3.8)	−2.02	−1.75, −1.19

[a] Absorption in ethanol. [b] Film cast on a Pt plate, measured in a CH<sub>2</sub>Cl<sub>2</sub> solution of (Et<sub>4</sub>N)BF<sub>4</sub> (0.1 M). The sweep rate was 50 mV s<sup>−1</sup>.  $E_{\text{pc}}$  = Peak cathode potential versus Ag<sup>+</sup>/Ag.  $E_{\text{pa}}$  = Peak anode potential versus Ag<sup>+</sup>/Ag.

azepinoazepines, and the absorptions of **3i** with non-aromatic substituents lie at the shortest wavelength among the azepinoazepine dichlorides. These data suggest that the  $\pi$ -conjugation system is expanded from the azepinoazepine ring to the aromatic N substituents. The observation of the absorption of **3b** at a wavelength longer than that of **3c** is explained by the steric effect of the methyl group at the 2-position of the 2,5-dimethylphenyl ring that may hinder the expansion of the  $\pi$ -conjugation system.

Cyclic voltammetry measurements suggested that the film of the azepinoazepines cast on a Pt plate underwent two-step electrochemical reduction of the azepinoazepine ring in a dichloromethane solution containing 0.1 M (NEt<sub>4</sub>)BF<sub>4</sub>. The electrochemical data also are summarized in Table 2. Azepinoazepines **3e–3g** with N-halophenyl substituents showed two reduction peaks, which were coupled with anodic peaks  $E_{\text{pa}}(1)$  and  $E_{\text{pa}}(2)$ . Although the peaks attributed to the two-step electrochemical reduction of the other azepinoazepines **3a–3d**, **3h**, and **3i** were duplicated, the two anodic peaks were separately observed. The reduction potential was dependent on the N substituent; product **3i** with its electron-donating *n*-hexyl substituents (Table 2, entry 9) showed a peak at higher reduction potential as compared to **3d–3g**, which have electron-withdrawing substituents (entries 4–7). The yellow film of the azepinoazepines changed to green after the electrochemical reduction and returned to yellow after crossing the  $E_{\text{pa}}(2)$  peak.

Scheme 2 shows a plausible reaction mechanism for formation of the N-substituted azepinoazepine dichlorides. The nucleophilic addition of an amine to the pyridinium rings of **1** occurs first to provide the intermediate **4**. Subsequently, ring opening of the dihydropyridyl rings of **4** gives an



**Scheme 2.** Possible reaction mechanism for the formation of N-substituted azepinoazepine dichlorides **3**.

intermediate **5**, which undergoes cyclization by elimination of 2,4-dinitroaniline (DNA) to provide **3**.

The product from expansion of one pyridinium ring of **1** was not obtained. On the other hand, nucleophilic addition of the NH group of the intermediate **5** to **1** followed by ring opening of the dihydropyridyl ring and elimination of 2,4-dinitroaniline may yield N-substituted diaza[13]annulenoannulene tetrachloride. However, such a product is not formed in the reaction of **1** with **2** as the lower basicity of the NH group of the intermediate **5** prevents nucleophilic addition to the pyridinium ring. These results indicate that the nucleophilic addition of an amine to the pyridyl group is a crucial step for the generation of the azepinoazepine ring.

In conclusion, N-substituted azepinoazepines were obtained in high yields by the one-pot reaction of **1** with amines.  $^1\text{H}$  NMR spectra of the products revealed that the  $\pi$  electrons are delocalized along the azepinoazepine ring. Cyclic voltammetry analysis indicated that the azepinoazepines are electrochemically active in films, and the electrochemical reaction was accompanied by electrochromism. Polymerization of **1** with aromatic diamines could provide  $\pi$ -conjugated polymers with the azepinoazepine ring in the main chain. In addition, the azepinoazepines **3d–3g** with 4-halophenyl substituents could be useful starting materials for functional compounds and polymers. These topics are currently under investigation in our laboratory.

## Experimental Section

**Representative procedure.** Preparation of **3a** in EtOH (Table 1, entry 1): 1,1'-Bis(2,4-dinitrophenyl)-4,4'-bipyridinium dichloride (**1**; 1.12 g, 2.0 mmol) and aniline (**2a**; 0.37 g, 4.0 mmol) were dissolved in dry ethanol (8 mL) under  $\text{N}_2$ . The solution was heated at reflux for 12 h under nitrogen, and then the brown precipitate from the reaction solution was separated by filtration. The precipitate was washed with acetone (150 mL) and dried under vacuum to give the title compound **3a** (0.59 g, 77%) as a brown solid. Compound **3a** was also obtained from the filtrate: Evaporation of the solvent from the filtrate gave a brown solid, which was washed with acetone (150 mL) and dried in vacuo to further afford compound **3a** (0.11 g, 14%). Total yield: 91%.

**Preparation of 3a in water** (Table 1, entry 2): An aqueous solution (4 mL) of **1** (0.56 g, 1.0 mmol) and **2a** (0.19 g, 2.0 mmol) was heated at reflux for 12 h, and then the 2,4-dinitroaniline precipitated from the reaction solution was filtered. Evaporation of water gave a brown solid, which was washed with acetone (150 mL) and dried under vacuum to afford compound **3a** (0.29 g, 75%).  $^1\text{H}$  NMR (400 MHz,  $\text{D}_2\text{O}$ ):  $\delta$  = 9.30 (d,  $J$  = 7.2 Hz, 4H), 8.67 (d,  $J$  = 7.2 Hz, 4H), 7.63–7.73 ppm (m, 10H);  $^{13}\text{C}$  NMR (100 MHz,  $[\text{D}_6]\text{DMSO}$ ):  $\delta$  = 148.9, 146.0, 142.2, 131.6, 130.2, 126.7, 124.8 ppm. FAB-MS:  $m/z$  345  $[\text{M}-\text{Cl}]^-$ , 310  $[\text{M}-2\text{Cl}]^-$ ; elemental analysis (%)

calcd for  $\text{C}_{22}\text{H}_{18}\text{N}_2\text{Cl}_2 \cdot 1.5\text{H}_2\text{O}$ : C 64.71, H 5.18, N 6.86; found: C 64.86, H 5.13, N 6.40.

Received: January 13, 2007

Published online: ■ ■ ■ ■, 2007

**Keywords:** amines · annulenes · fused-ring systems · nitrogen heterocycles · ring expansion

- a) H. V. Wikström, M. M. Mensonides-Harsema, T. I. F. H. Cremers, E. K. Moltzen, J. Arnt, *J. Med. Chem.* **2002**, *45*, 3280–3285; b) R. A. Cunha, J. E. Coelho, A. R. Costenla, L. V. Lopes, A. Parada, A. de Mendonça, A. M. Sebastião, J. A. Ribeiro, *Pharmacol. Toxicol.* **2002**, *90*, 208–213; c) A. Link, C. Kunick, *J. Med. Chem.* **1998**, *41*, 1299–1305; d) T. D. Boer, F. Neffkens, A. van Helvoirt, A. M. L. van Delft, *J. Pharmacol. Exp. Ther.* **1996**, *277*, 852–860; e) N. Haddjeri, P. Blier, C. D. Montiguy, *J. Pharmacol. Exp. Ther.* **1996**, *277*, 861–871; f) T. D. Boer, *J. Clin. Psychiatry* **1996**, *57*, 19–25.
- Selected examples: a) A. F. Yépez, A. Palma, E. Stashenko, A. Bahsas, J. M. Amaro-Luis, *Tetrahedron Lett.* **2006**, *47*, 5825–5828; b) A. H. Lewin, J. Szweczyk, J. W. Wilson, F. I. Carroll, *Tetrahedron* **2005**, *61*, 7144–7152; c) J. I. Andrés, J. Alcázar, J. M. Alonso, A. Díaz, J. Fernández, P. Gil, L. Iturrino, E. Matesanz, T. F. Meert, A. Megens, V. K. Sipido, *Bioorg. Med. Chem. Lett.* **2002**, *12*, 243–248; d) K. Kumar, R. Kapoor, A. Kapur, M. P. S. Ishar, *Org. Lett.* **2000**, *2*, 2023–2025; e) C. Kunick, A. Link, *J. Heterocycl. Chem.* **1995**, *32*, 803–805.
- a) X. Beebe, V. Gracías, S. W. Djuric, *Tetrahedron Lett.* **2006**, *47*, 3225–3228; b) S. K. Chattopadhyay, S. P. Roy, D. Ghosh, G. Biswas, *Tetrahedron Lett.* **2006**, *47*, 6895–6898; c) V. Gracías, A. F. Gasiecki, S. W. Djuric, *Tetrahedron Lett.* **2005**, *46*, 9049–9052; d) J. S. Yadav, B. V. S. Reddy, M. K. Gunpta, A. Prabhakar, B. Jagadeesh, *Chem. Commun.* **2004**, 2124–2125; e) L. A. Arnold, W. Luo, R. K. Guy, *Org. Lett.* **2004**, *6*, 3005–3007; f) K. H. Bleicher, F. Gerber, Y. Wüthrich, A. Alanine, A. Capretta, *Tetrahedron Lett.* **2002**, *43*, 7687–7690; g) B. H. Yang, S. L. Buchwald, *Org. Lett.* **1999**, *1*, 35–38.
- a) H. Cho, K. Murakami, H. Nakanishi, A. Fujisawa, H. Isoshita, M. Niwa, K. Hayakawa, Y. Hase, I. Uchida, H. Watanabe, K. Wakitani, K. Aisaka, *J. Med. Chem.* **2004**, *47*, 101–109; b) J. S. Yadav, C. Srinivas, *Tetrahedron* **2003**, *59*, 10325–10329; c) H.-S. Chong, B. Ganguly, G. A. Broker, R. D. Rogers, M. W. Brechbiel, *J. Chem. Soc. Perkin Trans. 1* **2002**, 2080–2086; d) H. Sawanishi, H. Muramatsu, T. Tsuchiya, *Chem. Commun.* **1990**, 628–630; e) T. K. Hansen, H. Thøgersen, B. S. Hansen, *Bioorg. Med. Chem. Lett.* **1997**, *7*, 2951–2954.
- I. Yamaguchi, Y. Gobara, M. Sato, *Org. Lett.* **2006**, *8*, 4279–4281.
- For recent reviews, see: a) C.-J. Li, *Chem. Rev.* **2005**, *105*, 3095–3165; b) U. M. Lindström, *Chem. Rev.* **2002**, *102*, 2751–2772.
- See Supporting Information.

## Communications

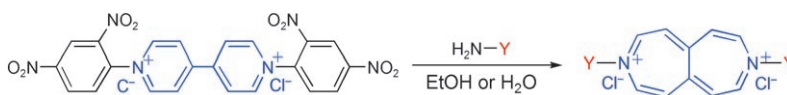


### Nitrogen Heterocycles

I. Yamaguchi,\* S. Tsutsui,  
M. Sato



Ring Expansion of a 4,4'-Bipyridyl  
Derivative into  $\pi$ -Conjugated  
Azepinoazepines



**Room to expand:** N-substituted azepinoazepines were obtained in high yields from 1,1'-bis(2,4-dinitrophenyl)-4,4'-bipyridinium dichloride with amines. The  $^1\text{H}$  NMR spectra of the products revealed

that  $\pi$  electrons were delocalized along the azepinoazepine ring, while cyclic voltammetry analysis indicated that the azepinoazepines were electrochemically active and electrochromic as thin films.